Independent PQ Control for Distributed Power Generation Systems under Grid Faults

P. Rodríguez[▲], A.V. Timbus[★], R. Teodorescu[★], M. Liserre[✷] and F. Blaabjerg[★]

[▲]Power Quality and Renewable Energy
Technical University of Catalonia
Barcelona - SPAIN
prodriguez@ee.upc.edu

[★]Institute of Energy Technology
Aalborg University
Aalborg - DENMARK
avt@iet.aau.dk

[✷]Electrotechnical and Electronic Eng. Dept.
Polytechnic of Bari
Bari - ITALY
liserre@poliba.it

***Abstract* – This work aims to present a generalized vector-based formulation for calculating the grid-side current reference of distributed power generation systems in order to independently control active and reactive power delivered to the grid. Strategies for current reference generation were implemented on the *abc* stationary reference frame and their effectiveness was demonstrated experimentally, perhaps validating the theoretical analysis even under grid fault conditions.**

I. INTRODUCTION

In the last fifteen years, the penetration of the wind turbine power generation is noticeably increased worldwide, i.e., from 7600 MW production in 1997 to 50000 MW at the end of 2005 and it will reach 180000 MW in 2010. This growing trend is stimulating the research in the power processing field aiming to optimize the energy extraction from the wind and the energy injection into the grid. As the wind penetration is increasing, the international standards are oriented to consider the wind turbine systems as classical generation system that should sustain the grid when necessary –mainly be faulty-active during short-circuits, do not contribute to the short-circuit power, have rolling capacity into the grid and generate/absorb reactive power [1]. These requirements make possible to foresee that the future standard wind systems will include a back-to-back converter. This would allow the full control on the power injected into the grid. Therefore, a wind generation system has to be able to 'ride through' a severe voltage dip or swell, as well as a frequency disturbance or other occurrences of deteriorated power quality.

The main problems that could lead a grid inverter to trip, under faulty grid operating conditions, are: under-/over-voltage and voltage oscillations in the dc-bus and over-currents due to distortion and imbalance [2]. However, while a grid inverter equipped with a well designed dc-bus voltage controller can sustain the dc-bus voltage and make it stiff respect to balanced dips, the effects due to imbalance both on the ac-side (current) and on the dc-side (dc voltage) are more dangerous. In fact, different grid disturbances should be treated in different ways. Many of the methods presented in literature propose a rigid constraint on the reference current that lead to inherent limitations such as reactive power oscillation [3] or impossibility to regulate the active and reactive powers independently [4][5].

On the contrary, this works aims to present a generalized vector-based formulation for current reference generation which can be applied on either the stationary or synchronous reference frame. In this work, these strategies have been implemented on the *abc* stationary reference frame.

II. CALCULATION OF CURRENT REFERENCES DELIVERING ACTIVE POWER

The instantaneous active power, p, supplied by a three-phase inverter to the grid is calculated by:

$$p = \mathbf{v} \cdot \mathbf{i}\,, \tag{1}$$

where $\mathbf{v} = (v_a, v_b, v_c) \in \mathbb{R}^3$ is the voltage vector in the point of common coupling (PCC), $\mathbf{i} = (i_a, i_b, i_c) \in \mathbb{R}^3$ is the injected current vector in such point, and '·' represents the dot product. Consequently, for a given voltage vector at the PCC, there exist infinite current vectors which are able to supply exactly same instantaneous active power to the grid.

In distributed generation systems, the instantaneous active power delivered by the energy source to the grid can be assumed as a constant throughout a grid period, *T*. Therefore, the reference of the instantaneous active power supplied by the front-end inverter of the back-to-back converter can be also considered a constant throughout each grid cycle, that is $p^* = P$. *Kirchhoff*'s current law guarantees that zero-sequence component of the currents in a three-phase three-wire system is always zero. In consequence, zero-sequence component of the grid voltage does not contribute to power transfer and it can be neglected in powers calculation. Thus, this study assumes that grid voltage used in equations, **v,** has been previously treated and only consists of positive- and negative-sequence components. Therefore, voltage and current vectors could be also expressed as $\mathbf{v} = (v_\alpha, v_\beta) \in \mathbb{R}^2$ and $\mathbf{i} = (i_\alpha, i_\beta) \in \mathbb{R}^2$, respectively.

Next paragraphs propose five different strategies to generate current references for the front-end inverter in order to deliver the active power *P* to the grid. In a first stage of this study, it has been supposed that no reactive power is injected into the grid, that is $q^* = 0$.

A. Instantaneous active-reactive control (IARC)

The most efficient set of currents delivering exactly the instantaneous active power *P* to the grid under generic voltage conditions can be calculated as follow [6][7]:

$$\mathbf{i}_p^* = g\,\mathbf{v} \quad ; \quad g = \frac{P}{|\mathbf{v}|^2}\,, \tag{2}$$

where $|\mathbf{v}|$ denotes the module –or collective value [7]– of the three-phase voltage vector, **v,** and g is the instantaneous conductance seen from the inverter output. Under balanced sinusoidal conditions, current references are perfectly sinusoidal since $|\mathbf{v}|$ –and so g– is constants. In presence of unbalanced grid faults however, $|\mathbf{v}|$ shows oscillations at twice the fundamental grid frequency due to the negative-sequence component of the faulty voltage. Consequently, the injected currents will not keep their sinusoidal waveform and high-order harmonics will appear in the current waveform during the grid fault. Current vector of (2) is instantaneously proportional to the voltage vector and so it does not have any orthogonal component in relation to the grid voltage, which gives rise to the injection of no reactive power to the grid.

Instantaneous power theories [6][7] allow identifying active and reactive components of the current for power delivery optimization –making reactive currents equal zero. However, when the quality of the current injected to the unbalanced grid becomes a major issue, it is necessary to establish certain constrains about how the current sequence-components and harmonics should be, even knowing that power delivery efficiency will decrease.

B. Instantaneously controlled positive-sequence (ICPS)

The instantaneous active power associated to an unbalanced current $\mathbf{i}=\mathbf{i}^{+}+\mathbf{i}^{-}$ which is injected in the PCC of a three-phase unbalanced grid with $\mathbf{v}=\mathbf{v}^{+}+\mathbf{v}^{-}$ is given by:

$$p=\mathbf{v}\cdot\mathbf{i}=\mathbf{v}^{+}\cdot\mathbf{i}^{+}+\mathbf{v}^{-}\cdot\mathbf{i}^{-}+\mathbf{v}^{+}\cdot\mathbf{i}^{-}+\mathbf{v}^{-}\cdot\mathbf{i}^{+}\,, \tag{3}$$

where superscripts '+' and '-' denote three-phase sinusoidal positive and negative-sequence signals, respectively.

From (3), positive-sequence current can be instantaneously controlled to deliver the active power P by imposing the following constrains in the current references calculation:

$$\mathbf{v}\cdot\mathbf{i}_p^{*+}=P\,, \tag{4a}$$

$$\mathbf{v}\cdot\mathbf{i}_p^{*-}=0\,. \tag{4b}$$

Expression of (4b) makes negative-sequence current components equal zero, whereas the positive-sequence current reference can be calculated from (4a) as follow:

$$\mathbf{i}_p^{*}=\mathbf{i}_p^{*+}+\mathbf{i}_p^{*-}=g^{+}\mathbf{v}^{+}\quad;\quad g^{+}=\frac{P}{\left|\mathbf{v}^{+}\right|^{2}+\mathbf{v}^{+}\cdot\mathbf{v}^{-}}\,. \tag{5}$$

According to the *p-q theory* [6], the instantaneous reactive power associated to the current vector of (5) is given by:

$$q=\left|\mathbf{v}\times\mathbf{i}_p^{*+}\right|=\underbrace{\left|\mathbf{v}^{+}\times\mathbf{i}_p^{*}\right|}_{0}+\underbrace{\left|\mathbf{v}^{-}\times\mathbf{i}_p^{*}\right|}_{\tilde{q}}\,. \tag{6}$$

where the sign '×' denotes the cross product. It is possible to appreciate in (6) how the current references calculated by means the *ICPS* strategy give rise to oscillations at twice the fundamental utility frequency in the instantaneous reactive power injected to the grid.

It is worth to notice that positive- and negative-sequence components of the grid voltage should be perfectly characterized to implement this –and next– control strategy. Therefore, a PLL capable of detecting voltage sequence components under unbalanced operating conditions should be added to the control system [8][9].

C. Positive- negative-sequence compensation (PNSC)

Active power P can be delivered to the grid injecting sinusoidal positive- and negative-sequence currents at the PCC. To achieve it, the following constrains should be imposed in the current references calculation:

$$\mathbf{v}^{+}\cdot\mathbf{i}_p^{*+}+\mathbf{v}^{-}\cdot\mathbf{i}_p^{*-}=P\,, \tag{7a}$$

$$\mathbf{v}^{+}\cdot\mathbf{i}_p^{*-}+\mathbf{v}^{-}\cdot\mathbf{i}_p^{*+}=0\,. \tag{7b}$$

From (7b) the negative-sequence reference current can be written as:

$$\mathbf{i}_p^{*-}=-g^{-}\mathbf{v}^{-}\quad;\quad g^{-}=\frac{\mathbf{v}^{+}\cdot\mathbf{i}_p^{*+}}{\left|\mathbf{v}^{+}\right|^{2}}\,. \tag{8}$$

Substituting (8) in (7a) and simplifying, the positive-sequence reference current can be calculated by:

$$\mathbf{i}_p^{*+}=g^{+}\mathbf{v}^{+}\quad;\quad g^{+}=\frac{P}{\left|\mathbf{v}^{+}\right|^{2}-\left|\mathbf{v}^{-}\right|^{2}}\,. \tag{9}$$

Adding (8) and (9), the final current references can be written as:

$$\mathbf{i}_p^{*}=\mathbf{i}_p^{*+}+\mathbf{i}_p^{*-}=g^{\pm}\left(\mathbf{v}^{+}-\mathbf{v}^{-}\right)\quad;\quad g^{\pm}=\frac{P}{\left|\mathbf{v}^{+}\right|^{2}-\left|\mathbf{v}^{-}\right|^{2}}\,. \tag{10}$$

Expression (10) indicates that injected current and voltage vectors have different directions. Consequently, the instantaneous reactive power delivered to the grid is not equal to zero but exhibits second-order oscillations given by:

$$q=\left|\mathbf{v}\times\mathbf{i}_p^{*}\right|=\underbrace{\left|\mathbf{v}^{+}\times\mathbf{i}_p^{*+}\right|+\left|\mathbf{v}^{-}\times\mathbf{i}_p^{*-}\right|}_{0}+\underbrace{\left|\mathbf{v}^{+}\times\mathbf{i}_p^{*-}\right|+\left|\mathbf{v}^{-}\times\mathbf{i}_p^{*+}\right|}_{\tilde{q}}\,. \tag{11}$$

D. Average active-reactive control (AARC)

During unbalanced grid faults, current references obtained by means of the *IARC* strategy present high order harmonics in their waveform because the instantaneous conductance, g, does not remain constant throughout the grid period, T. Since P has been assumed as a constant, such harmonics come from the second-order component of $|\mathbf{v}|^{2}$, being:

$$|\mathbf{v}|^{2}=\left|\mathbf{v}^{+}\right|^{2}+\left|\mathbf{v}^{-}\right|^{2}+2\left|\mathbf{v}^{+}\right|\left|\mathbf{v}^{-}\right|\cos\left(2\omega t+\phi^{+}-\phi^{-}\right). \tag{12}$$

High-order harmonics in the current references will be cancelled if they are calculated by:

$$\mathbf{i}_p^{*}=G\,\mathbf{v}\quad;\quad G=\frac{P}{V_{\Sigma}^{2}}\,, \tag{13}$$

where V_{Σ} is the collective rms value of the grid voltage and it is defined by:

$$V_{\Sigma}=\sqrt{\frac{1}{T}\int_{0}^{T}|\mathbf{v}|^{2}\,dt}=\sqrt{\left|\mathbf{v}^{+}\right|^{2}+\left|\mathbf{v}^{-}\right|^{2}}\,. \tag{14}$$

In this case, instantaneous conductance is a constant under periodic conditions, namely g=G. *Buchholz* [10], a precursor of the study on the time-domain of active and non-active currents in poly-phase systems, proved that, for a given grid voltage **v**, the current references calculated by (13) lead to the smallest possible collective rms value of such currents, I_{Σ}, delivering the electrical energy $P \cdot T$ over one grid period. The lower value of I_{Σ}, the lower conduction losses in the system and the higher efficiency.

Current vector of (13) has the same direction that the grid voltage vector and so it will not give rise to any reactive power. However, the instantaneous active power delivered to the unbalanced grid will not equal *P* but it will be given by:

$$p = \mathbf{i}_p^* \cdot \mathbf{v} = \frac{|\mathbf{v}|^2}{V_{\Sigma}^2} P = P + \tilde{p}\,. \tag{15}$$

Substituting (12) and (14) in (15) it is easy to justify that instantaneous active power delivered to the unbalanced grid consists of a mean value *P* accompanied by oscillations $\tilde{p}$ at twice the grid frequency. Since *G* is a constant, voltage and current waveforms will be monotonously proportional.

E. Balanced positive-sequence (BPS)

When the quality of the currents injected in the grid plays a decisive role they can be calculated as:

$$\mathbf{i}_p^* = G^+ \mathbf{v}^+ \quad ; \quad G^+ = \frac{P}{|\mathbf{v}^+|^2}, \tag{16}$$

Current vector of (16) consists of a set of perfectly balanced positive-sequence sinusoidal waveforms. Under unbalance operating conditions, the instantaneous active power delivered to the grid will differ from *P* because of the interaction between the positive-sequence injected current and the negative-sequence grid voltage, that is:

$$p = \mathbf{v} \cdot \mathbf{i}_p^* = \underbrace{\mathbf{v}^+ \cdot \mathbf{i}_p^*}_{P} + \underbrace{\mathbf{v}^- \cdot \mathbf{i}_p^*}_{\tilde{p}}, \tag{17}$$

where $\tilde{p}$ is power oscillation at twice the fundamental utility frequency. Likewise, the instantaneous reactive power can be calculated as:

$$q = |\mathbf{v} \times \mathbf{i}_p^*| = \underbrace{|\mathbf{v}^+ \times \mathbf{i}_p^*|}_{0} + \underbrace{|\mathbf{v}^- \times \mathbf{i}_p^*|}_{\tilde{q}}, \tag{18}$$

where $\tilde{q}$ is also oscillating at twice the fundamental utility frequency.

Positive and negative-sequence vectors studied in this section can be considered as orthogonal –seen over one grid period– and represented on a Euclidean plane $\mathbb{R}^2$ since their scalar product throughout the grid period is always equal to zero, that is:

$$\overline{\mathbf{x}^+ \cdot \mathbf{y}^-} = \frac{1}{T}\int_0^T \mathbf{x}^+ \cdot \mathbf{y}^- dt = 0\,, \tag{19}$$

This graphic representation of voltage and current vectors is shown in Fig. 1 and allows a better understanding of previous strategies for current reference generation.

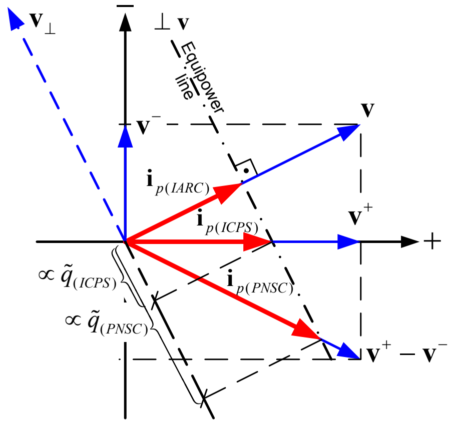

Fig. 1. Positive- and negative-sequence Euclidean plane.

For a better visualization and understanding, only current vectors from *IARC*, *ICPS*, and *PNSC* strategies have been represented in Fig. 1. Amplitude of all three current vectors is delimited by the ‘equipower line’, which is perpendicular to **v**. Amplitude of oscillations in the instantaneous reactive power associated to each strategy, $\tilde{q}$, is proportional to the projection of its current vector over the equipower line. Current vectors from *AARC* and *BPS* strategies have the same direction that those vectors from *IARC* and *ICPS* strategies, respectively. However, their amplitudes are not instantaneously controlled, generating oscillations in the active power. None of these strategies give rise to a finite mean value in the reactive power injected to the grid.

III. EVALUATION OF CONTROL STATEGIES DELIVERING ACTIVE POWER TO THE GRID

The above control strategies have been implemented in an experimental setup comprising a current-controlled VSI and an LC filter (L = 10mH; C = 0.7μF per phase) connected to the grid through a Δy transformer. The faulty grid is here replaced by a programmable three-phase ac-power source. A dSpace 1103 DSP card is used to implement a dead-beat current controller, the PLL for detecting positive- and negative-sequence voltage components, and the algorithm to calculate the current references on natural *abc* reference frame. The sampling and switching frequencies are set to 15 kHz. Since the ac-power source cannot accept power, a resistive local load has been connected to the system. The dc-link controller has been relaxed in order to not influence the creation of the current references. As a consequence, dc-power sources are used to supply the necessary dc-link voltage, which was set to 700 V.

Connected to the Δ winding of the transformer, the programmable ac-power source suddenly decreases the rms voltage of one phase from 220V to 100V, generating a dip type B with a characteristic voltage $V_B = 0.454$ pu. This single-phase fault is propagated to the y winding of the transformer as a dip type C with a characteristic voltage $V_C = 0.636$ pu [11]. It implies that positive- and negative-sequence phasors during the fault are given by

$\vec{V}^{+} = 0.818\underline{|0^{\circ}}$ pu and $\vec{V}^{-} = 0.182\underline{|0^{\circ}}$ pu , being the pre-fault voltage $\vec{V}^{+}_{pf} = 1\underline{|0^{\circ}}$ pu . The power delivered to the grid was P=1.5kW and Q=0.

Fig. 3 shows characteristics waveforms for the five previously presented control strategies. It is worth to say that experimental waveforms slightly differ from the theoretical ones because of the non-idealities of the inverter and grid, imperfections in the control, and sensing errors. However, these current and power plots properly ratify the conclusions of the theoretical study of § II.

To evaluate waveforms of Fig. 3 some characteristic indicators has been calculated and represented in Fig. 2. Data to calculate such indicators come from a simulation model carefully adjusted to reflect the behaviour of the actual experimental plant. Normalized in respect to its pre-fault value, the current collective rms value is calculated according to (14) and represented in Fig. 2(a). Collective rms values of current and voltage allow calculating the effective apparent power, $S_e = V_{\Sigma} I_{\Sigma}$. According to [12], S_e allows rational and correct computation of the power factor for sinusoidal unbalanced or for non-sinusoidal balanced or unbalanced situations. Therefore, the effective power factor [12], $P_{Fe} = P/S_e$, is calculated and represented in Fig. 2(b). This figure shows how PNSC is the least efficient strategy whereas AARC is the most. THD of a current waveform can be calculated as:

$$THD(\%) = \frac{1}{I_{(1)}} \sqrt{I^2_{RMS} - I^2_{(1)}} \cdot 100 \,. \qquad (20)$$

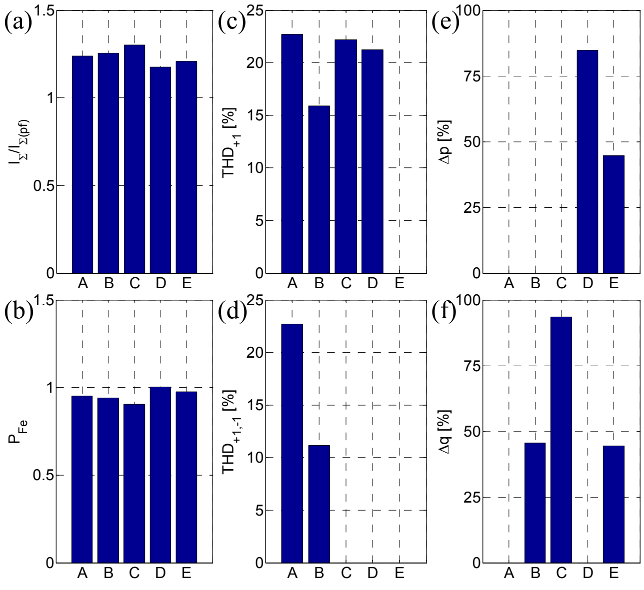

Fig. 2. Characteristic indicators of current reference generation strategies. [A-(IARC), B-(ICPS), C-(PNSC), D-(AARC), E-(BPS)].

In this work, overall current quality of the three-phase system will be evaluated by means of (20) but using collective instead of individual rms values. Moreover, in our unbalanced system can exist two fundamental frequency currents with opposite sequences. For this reason, two collective values of THD are calculated. Fig. 2(c) represents THD$_{+1}$, calculated assuming that the current component at fundamental frequency should be only positive-sequence.

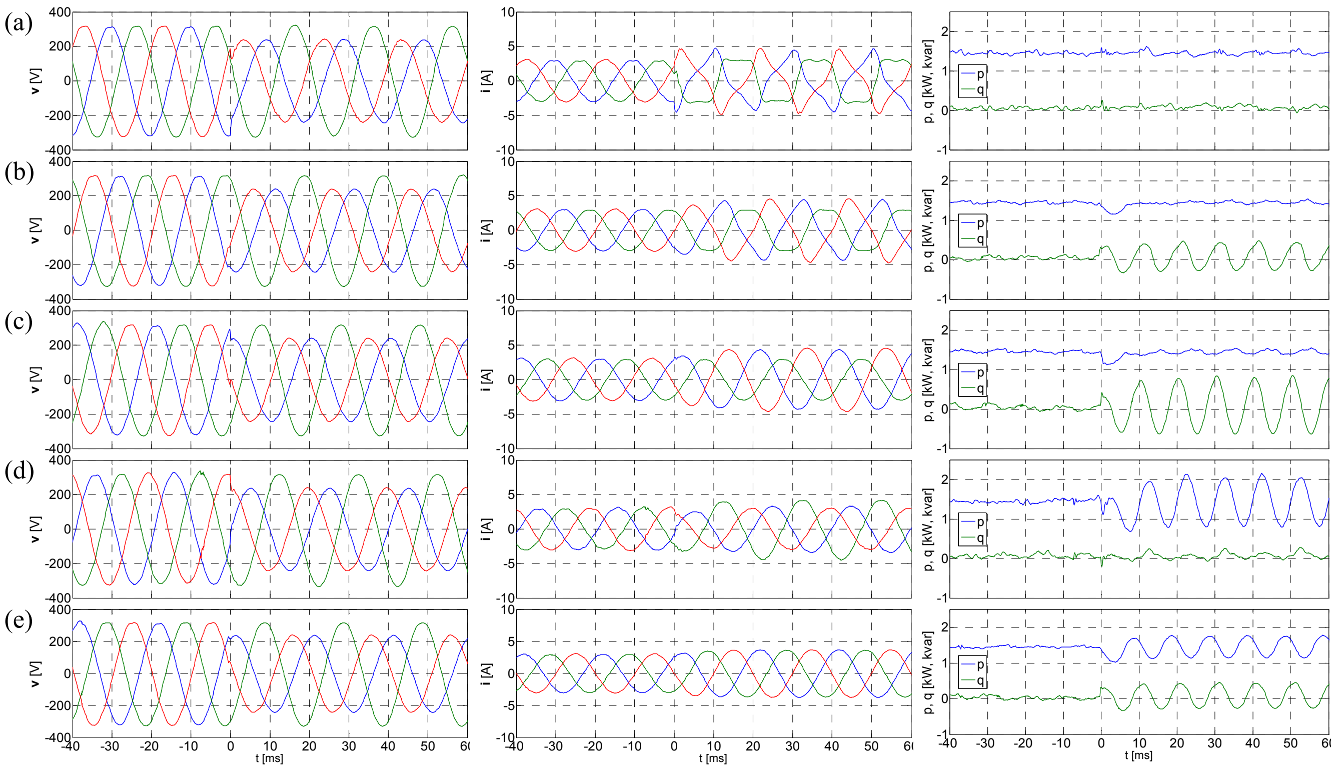

Fig. 3. Experimental results applying current reference strategies with P=1.5kW and Q=0. Columns from left to right: faulty grid voltage, injected currents, instantaneous active and reactive delivered power. (a) IARC, (b) ICPS, (c) PNSC, (d) AARC, and (e) BPS.

Fig. 2(d) represents $THD_{+1,-1}$, calculated assuming that current at fundamental frequency can consist of positive- and negative-sequence components. In these current quality plots, BPS strategy obtains the best results and IARC the worst. Fig. 2(e) represents the amplitude of the instantaneous active power oscillations referred to S_e. These active power oscillations are automatically reflected as voltage oscillations in the dc-bus of the inverter. Strategies with a poor currents quality give rise to the smallest active power oscillations. Fig. 2(f) shows the amplitude of the instantaneous reactive power oscillations referred to S_e. These oscillations, moreover to generate unnecessary power losses and voltage drops, reduce the operating margin of the inverter.

IV. CALCULATION OF CURRENT REFERENCES DELIVERING REACTIVE POWER

In earlier control strategies, active current reference and voltage vectors with the same sequence and frequency had always the same direction. Therefore, the instantaneous reactive power injected in the grid by means of such strategies was entirely oscillatory and its mean value over a grid cycle was always equal zero. This section is devoted to find a reactive current vector, $\mathbf{i}_q$, which is in-quadrature with the voltage vector $\mathbf{v}$ and injects the following instantaneous reactive power to the grid:

$$q = \left|\mathbf{v} \times \mathbf{i}_q\right| = \mathbf{v}_\perp \cdot \mathbf{i}_q . \tag{21}$$

In (21), $\mathbf{v}_\perp$ is an imaginary 90-degree leaded version of the voltage vector $\mathbf{v}$, see Fig. 1

Following the same reasoning as in § II, five control strategies can be proposed to calculate the reactive current references. Without repeating all the analysis steps, such control strategies are formulated in the following, being b the instantaneous susceptance seen from output of the inverter.

A. Instantaneous active-reactive control (IARC)

$$\mathbf{i}_q^* = b\,\mathbf{v}_\perp \quad ; \quad b = \frac{Q}{\left|\mathbf{v}\right|^2} \tag{22}$$

B. Instantaneously controlled positive-sequence (ICPS)

$$\mathbf{i}_q^* = b^+ \mathbf{v}_\perp^+ \quad ; \quad b^+ = \frac{Q}{\left|\mathbf{v}^+\right|^2 + \mathbf{v}^+ \cdot \mathbf{v}^-} \tag{23}$$

C. Positive- negative-sequence compensation (PNSC)

$$\mathbf{i}_q^* = b^\pm \left(\mathbf{v}_\perp^+ - \mathbf{v}_\perp^-\right) \quad ; \quad b^\pm = \frac{Q}{\left|\mathbf{v}^+\right|^2 - \left|\mathbf{v}^-\right|^2} \tag{24}$$

D. Average active-reactive control (AARC)

$$\mathbf{i}_q^* = B\,\mathbf{v}_\perp \quad ; \quad B = \frac{Q}{V_\Sigma^2} \tag{25}$$

E. Balanced positive-sequence (BPS)

$$\mathbf{i}_q^* = B^+ \mathbf{v}_\perp^+ \quad ; \quad B^+ = \frac{Q}{\left|\mathbf{v}^+\right|^2} \tag{26}$$

Using the same experimental setup as previously, reactive and active strategies were evaluated together delivering P=1.5kW and Q=1.3kvart to the grid. Fig. 4 shows characteristics waveforms obtained from such evaluation.

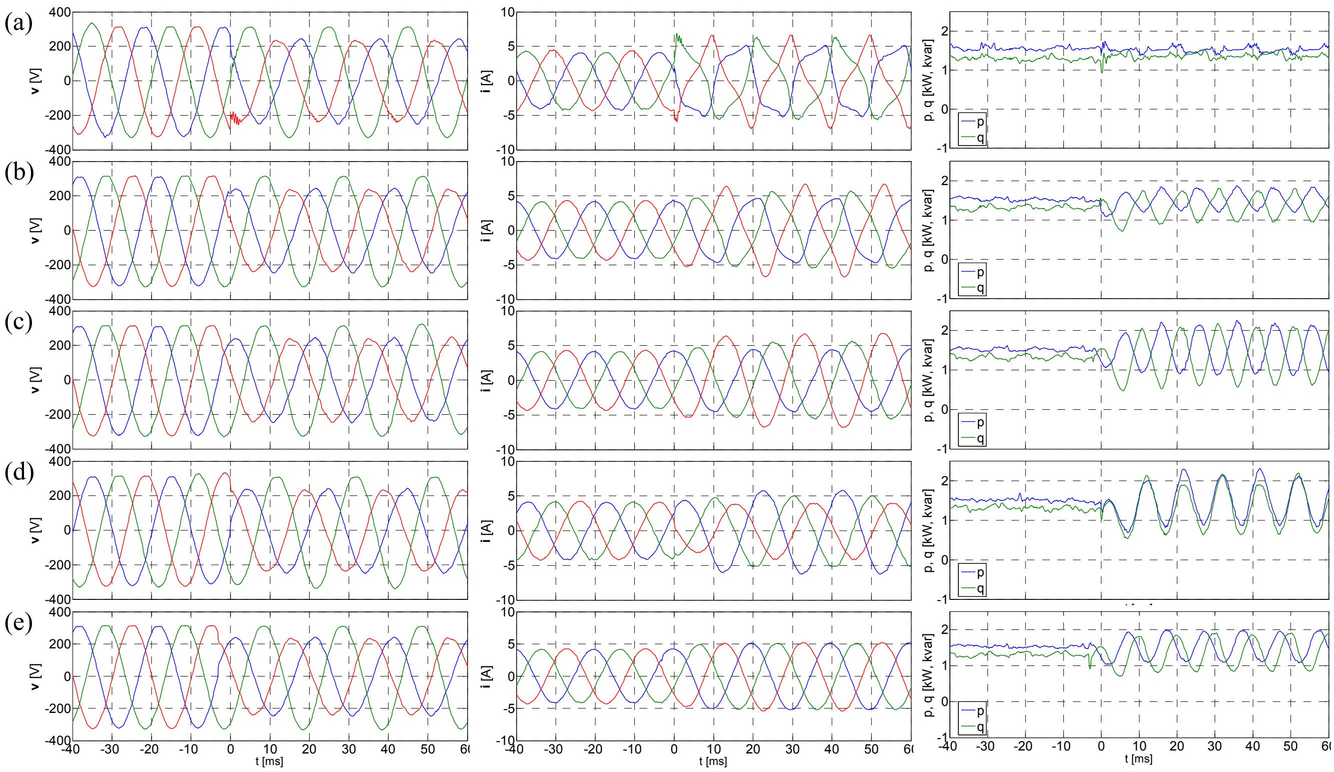

Fig. 4. Experimental results applying current reference strategies with P=1.5kW and Q=1.3kvar. Columns from left to right: faulty grid voltage, injected currents, instantaneous active and reactive delivered power. (a) IARC, (b) ICPS, (c) PNSC, (d) AARC, and (e) BPS.

Once more, experimental waveforms of Fig. 4 slightly differ from the theoretical ones because of the non-idealities of the experimental setup. In this experiment, the algorithm to calculate current references was implemented on natural *abc* reference frame and so the orthogonal voltage vector was calculated by:

$$\mathbf{v}_{\underset{(abc)}{\perp}} = \left[T_\perp\right]\mathbf{v}_{(abc)} \quad ; \quad \left[T_\perp\right] = \frac{1}{\sqrt{3}}\begin{bmatrix} 0 & -1 & 1 \\ 1 & 0 & -1 \\ -1 & 1 & 0 \end{bmatrix} \tag{27}$$

Current references of Fig. 4 result from a peer-to-peer combination of the previously exposed strategies to control the active and reactive power delivered to the grid, e.g., the reference current in Fig. 4(a) was calculated as:

$$\mathbf{i}^* = \mathbf{i}_p^* + \mathbf{i}_q^* = g\ \mathbf{v} + b\ \mathbf{v}_\perp\,, \tag{28}$$

however, any other combination of active and reactive terms could be also possible.

Analysis of the waveforms of Fig. 4 conducts to similar conclusions to those obtained when the characteristic indicators of Fig. 2 were discussed. The only remarkable difference is related to the oscillations in instantaneous powers. Fig. 4 evidences that only *IARC* strategy is able to keep constant the delivered instantaneous active and reactive powers when grid voltage is unbalanced. The rest of strategies present additional power oscillations given by:

$$\begin{aligned} ICPS: P &= \mathbf{v}^+ \cdot \mathbf{i}_p^* \ ; \ \tilde{p} = \mathbf{v}^- \cdot \mathbf{i}_q^* \\ Q &= \left|\mathbf{v}^+ \times \mathbf{i}_q^*\right| \ ; \ \tilde{q} = \left|\mathbf{v}^- \times \mathbf{i}_p^*\right| \end{aligned} \tag{29}$$

$$\begin{aligned} PNSC: P &= \mathbf{v}^+ \cdot \mathbf{i}_p^{*+} + \mathbf{v}^- \cdot \mathbf{i}_p^{*-} \ ; \ \tilde{p} = \mathbf{v}^+ \cdot \mathbf{i}_q^{*-} + \mathbf{v}^- \cdot \mathbf{i}_q^{*+} \\ Q &= \left|\mathbf{v}^+ \times \mathbf{i}_q^{*+}\right| + \left|\mathbf{v}^- \times \mathbf{i}_q^{*-}\right| ; \tilde{q} = \left|\mathbf{v}^+ \times \mathbf{i}_p^{*-}\right| + \left|\mathbf{v}^- \times \mathbf{i}_p^{*+}\right| \end{aligned} \tag{30}$$

$$\begin{aligned} AARC: p &= \mathbf{i}_p^* \cdot \mathbf{v} = \frac{|\mathbf{v}|^2}{V_\Sigma^2} P = P + \tilde{p} \\ q &= \mathbf{i}_q^* \cdot \mathbf{v} = \frac{|\mathbf{v}|^2}{V_\Sigma^2} Q = Q + \tilde{q} \end{aligned} \tag{31}$$

$$\begin{aligned} BPS: P &= \mathbf{v}^+ \cdot \mathbf{i}_p^* \ ; \ \tilde{p} = \mathbf{v}^- \cdot \left(\mathbf{i}_p^* + \mathbf{i}_q^*\right) \\ Q &= \left|\mathbf{v}^+ \times \mathbf{i}_q^*\right| \ ; \ \tilde{q} = \left|\mathbf{v}^- \times \left(\mathbf{i}_p^* + \mathbf{i}_q^*\right)\right| \end{aligned} \tag{32}$$

XI. CONCLUSION

This paper has presented and discussed five strategies to generate the current references for grid-connected inverters in order to independently control the active and reactive power delivered to the grid under unbalanced operating conditions. Study carried out in this work is completely general and strategies for generating current reference can be implemented on either the stationary or synchronous reference frame.

Hypotheses and assumptions adopted in the theoretical study of the strategies are ratified by simulation and experimental results. In the experimental setup, current control strategies were programmed on the *abc* stationary reference frame.

X. ACKNOWLEDGMENT

This work was supported by Ministerio de Ciencia y Tecnologia of Spain under Project ENE2004-07881-C03-02.

XI.- REFERENCES

[1] P.B. Eriksen, T. Ackermann, H. Abildgaard, P. Smith, W. Winter and J.M. Rodriguez, "System operation with high wind penetration," *IEEE Power and Energy Magazine*, vol.3, pp. 65- 74, Nov./Dec. 2005.

[2] L. Moran, P. D. Ziogas and G. Joos: "Design aspects of synchronous PWM rectifier-inverter system under unbalanced input voltage conditions", *IEEE Trans. on Ind. Applicat.*, vol. 28, Nov./Dec. 1992, pp. 1286-1293.

[3] A.V. Stankovic and T.A. Lipo, "A novel control method for input output harmonic elimination of the PWM boost type rectifier under unbalanced operating conditions," *IEEE Trans. on Power Electron.*, vol. 16, pp. 603-611, Sept. 2001.

[4] H-S. Song and K. Nam, "Dual current control scheme for PWM converter under unbalanced input voltage conditions," *IEEE Trans. on Ind. Electron.*, vol. 46, pp. 953-959, Oct. 1999.

[5] P. Rioual, H. Pouliquen, J.-P. Louis, "Regulation of a PWM rectifier in the unbalanced network state using a generalized model," *IEEE Trans. on Power Electron.*, vol.11, pp.495-502, May 1996.

[6] H. Akagi, Y. Kanazawa, and A. Nabae, "Instantaneous reactive power compensator comprising switching devices without energy storage components," *IEEE Trans. on Ind. Applicat.*, vol. IA-20, pp. 625-630, May/June 1984.

[7] M. Depenbrock, V. Staudt, and H. Wreder, "A theoretical investigation of original and modified instantaneous power theory applied to four-wire systems," *IEEE Trans. Ind. Applicat.*, vol. 39, pp. 1160-1167, July/Aug. 2003.

[8] P. Rodríguez, J. Pou, J. Bergas, I. Candela, R. Burgos, and D. Boroyevich, "Double synchronous reference frame PLL for power converters," *in Proc. IEEE Power Electron. Spec. Conf. (PESC'05)*, 2005, pp. 1415-1421.

[9] A. V. Timbus, P. Rodríguez, R. Teodorescu, M. Liserre and F. Blaabjerg, "Control strategies for distributed power generation systems operating on faulty grid," *in Proc. IEEE Int. Symp. Ind. Electron. (ISIE'06)*, 2006.

[10] F. Buchholz, "Das Begriffsystem Rechtleistung. Wirkleistung, totale Blindleistung," Munich, Germany: Selbstverlag, 1950.

[11] A. Sannino, M.H.J. Bollen, J. Svensson, "Voltage tolerance testing of three-phase voltage source converters," *IEEE Trans. Power Delivery*, vol. 20, Apr. 2005, pp. 1633-1639.

[12] IEEE Standard 1459-2000: *IEEE Trial-Use Standard Definitions for Power Measurement of Electric Power Quantities Under Sinusoidal, Nonsinusoidal, Balanced or Unbalanced Conditions.* IEEE, 21 June 2000. Upgraded to full-use December 2002.